

AD-A062 452

AIR FORCE GEOPHYSICS LAB HANSCOM AFB MASS

F/G 17/5

SWIR-MWIR ELECTRON FLUORESCENCE MEASUREMENTS IN N2/O2 AND AIR.(U)

APR 78 B D GREEN, G E CALEDONIA, R E MURPHY

UNCLASSIFIED

AFOL-TR-78-0083

DNA-HAES-76

NL

| OF |

AD
A062452



END

DATE

FILMED

3-79

DDC

(12) LEVEL II

AFGL-TR-78-0083

ENVIRONMENTAL RESEARCH PAPERS, NO. 629
HAES NO. 76

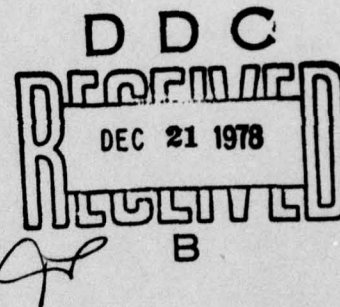


AD A062452

SWIR-MWIR Electron Fluorescence Measurements in N_2/O_2 and Air

B. D. GREEN
G. E. CALEDONIA
R. E. MURPHY

4 April 1978



Approved for public release; distribution unlimited.

This research was sponsored by the Defense Nuclear Agency under Subtask 125BAXHX632, Work Unit 07, entitled "LABCEDE Investigations of Irradiated N_2 , O_2 and Other Gaseous Mixtures."

OPTICAL PHYSICS DIVISION PROJECT 2310
AIR FORCE GEOPHYSICS LABORATORY
HANSCOM AFB, MASSACHUSETTS 01731

AIR FORCE SYSTEMS COMMAND, USAF



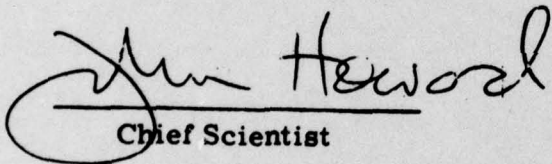
78 12 18 158

DDC FILE COPY

This report has been reviewed by the ESD Information Office (OI) and is releasable to the National Technical Information Service (NTIS).

This technical report has been reviewed and is approved for publication.

FOR THE COMMANDER


Chief Scientist

Qualified requestors may obtain additional copies from the Defense Documentation Center. All others should apply to the National Technical Information Service.

(18) DNA

(19) HAES-76

(9) Environmental research papers

Unclassified

SECURITY CLASSIFICATION OF THIS PAGE (When Data Entered)

REPORT DOCUMENTATION PAGE		READ INSTRUCTIONS BEFORE COMPLETING FORM
1. REPORT NUMBER	2. GOVT ACCESSION NO.	3. RECIPIENT'S CATALOG NUMBER
AFGL-TR-78-0083, AFGL-ERP-629		
4. TITLE	5. TYPE OF REPORT & PERIOD COVERED	
SWIR-MWIR ELECTRON FLUORESCENCE MEASUREMENTS IN N ₂ /O ₂ AND AIR	Scientific, Interim.	
6. AUTHOR(s)	7. PERFORMING ORG. REPORT NUMBER	
B. D. Green G. E. Caledonia R. E. Murphy	ERP No. 629	
8. PERFORMING ORGANIZATION NAME AND ADDRESS	9. CONTRACT OR GRANT NUMBER(s)	
Air Force Geophysics Laboratory (OPR-1) Hanscom AFB, Massachusetts 01731	HAES No. 76	
10. CONTROLLING OFFICE NAME AND ADDRESS	11. PROGRAM ELEMENT, PROJECT, TASK, AREA & WORK UNIT NUMBERS	
Air Force Geophysics Laboratory (OPR-1) Hanscom AFB, Massachusetts 01731	61102F 2310G401	
12. REPORT DATE	13. NUMBER OF PAGES	
4 April 1978	31	
14. MONITORING AGENCY NAME & ADDRESS (if different from Controlling Office)	15. SECURITY CLASS. (of this report)	
	Unclassified	
16. DISTRIBUTION STATEMENT (of this Report)		
Approved for public release; distribution unlimited.		
17. DISTRIBUTION STATEMENT (of the abstract entered in Block 20, if different from Report)		
B		
18. SUPPLEMENTARY NOTES		
* Physical Sciences Inc., Woburn, MA This research was sponsored by the Defense Nuclear Agency under Subtask I25BAXHX632, Work Unit 07, entitled "LABCEDE Investigations of Irradiated N ₂ , O ₂ and Other Gaseous Mixtures."		
19. KEY WORDS (Continue on reverse side if necessary and identify by block number)		
Fluorescence Electron irradiation Carbon dioxide Infrared Nitric oxide, OH, N ₂ O		
20. ABSTRACT (Continue on reverse side if necessary and identify by block number)		
The infrared fluorescence of electron irradiated room air and mixtures of N ₂ /O ₂ has been observed over the spectral range of 1600-6700/cm ⁻¹ . Dominant spectral features include the NO fundamental and first overtone bands as well as the CO ₂ (ν ₃) and N ₂ O(ν ₃) fundamental bands. Comparisons between the spectra observed in room air and laboratory N ₂ /O ₂ mixtures are provided.		

DD FORM 1 JAN 73 1473

EDITION OF 1 NOV 65 IS OBSOLETE

Unclassified

SECURITY CLASSIFICATION OF THIS PAGE (When Data Entered)

409 578

Am

627044

Preface

The authors would like to thank Dr. Charles Blank for his interest, advice, and support of the work presented. Support by the Defense Nuclear Agency, Atmospheric Effects Division, Subtask S99QAX-H1004-WU07, as part of the LABCEDE Program is acknowledged and appreciated.

I

ACCESSION for		
NTIS	White Section	<input checked="" type="checkbox"/>
DOC	Self Section	<input type="checkbox"/>
UNANNOUNCED		<input type="checkbox"/>
JUSTIFICATION		
BY		
DISTRIBUTION/AVAILABILITY CODES		
Dist.	AVAIL.	and/or SPECIAL
A		

PREVIOUS PAGE NOT FILLED
BLANK

78 12 18 158

Contents

1. INTRODUCTION	7
2. EXPERIMENTAL	9
3. DATA ANALYSES AND INTERPRETATION	12
4. SUMMARY AND CONCLUSIONS	25
REFERENCES	26

Illustrations

1. MWIR Fluorescence at Beam Termination From 80% N ₂ /20% O ₂ Mixtures at 100 Torr Pressure, for Slow-Flow Conditions	13
2. MWIR Fluorescence of Figure 1 at Beam Termination With 10 cm ⁻¹ Resolution	14
3. MWIR Fluorescence 0.2 msec After Beam Termination for the Same Run as Figure 2	15
4. MWIR Fluorescence at Beam Termination From Filtered Room Air at 100 Torr Pressure and Slow-Flow Conditions	16
5. Fluorescence 0.2 msec After Beam Termination for Conditions of Figure 4	16
6. Fluorescence at 3.4 msec After Beam Termination for Run of Figures 4 and 5	17

Illustrations

7. Uncalibrated Fluorescence Observed With PbS Detector at Beam Termination From Filtered Room Air Under Standard Slow-Flow Conditions	18
8. Comparison of SWIR Fluorescence with Synthetic Spectrum of NO	18
9. Spectrum of Filtered Room Air with Estimated CO ₂ and N ₂ O Bands Shown for Comparison	19
10. SWIR Fluorescence From 80% N ₂ /20% O ₂ Mixtures at 100 Torr Pressure Under Slow-Flow Conditions	20
11. Comparison of N ₂ /O ₂ and Room Air Spectra Taken Under Similar Conditions	20
12. SWIR Fluorescence From a Trace Oxygen Run Under Slow-Flow Conditions	22
13. SWIR Fluorescence 3.5 msec After Beam Termination for Run of Figure 12	22
14. Comparison of Synthetic Spectrum of OH With Spectral Features of Figure 13	23

SWIR - MWIR Electron Fluorescence Measurements in N_2/O_2 and Air

1. INTRODUCTION

One of the main topics of discussion at the recent High Altitude Effects Simulation (HAES) Infrared Data Review meeting¹ was the origin of, and data base for, 2.7 μm band radiation occurring in the quiescent and aurorally disturbed upper atmosphere. The short wave infrared data taken on several recent rocket flights were discussed and some comparisons with theoretical estimates were provided. These predictions were developed under the assumption that the dominant atmospheric radiation source in the 2.7 μm region is the NO first overtone vibration/rotation band. Although this thesis is generally accepted as valid, it has not yet been verified experimentally inasmuch as to date upper atmospheric fluorescence measurements have been performed utilizing radiometers which allow little spectral resolution.

It was pointed out during the meeting² that there are several sets of measurements of 2.7 μm radiation which are not consistent with an NO source. Specifically, in some instances measurements of the total columnar 2.7 μm radiation as a function of altitude exhibit a behaviour typical of an optically thick source, whereas

(Received for publication 3 April 1978)

1. Proceedings of the HAES Infrared Data Review, 13-15 June 1977, Falmouth, MA, AFGL Report OP-TM-05.
2. Proceedings of the HAES Infrared Data Review, 13-15 June 1977, AFGL Report OP-TM-05, pp 327-341, presented by H. Mitchell.

atmospheric NO is optically thin. Furthermore it was pointed out that the ratio of 2.7 μm to 5.3 μm band radiation observed in recent project EXCEDE measurements³ was much too large to be explained in terms of the ratio of the NO first overtone to fundamental band radiation. Lastly, some laboratory measurements of electron irradiated air⁴ were shown to exhibit spectral features due to a species other than NO.

Of course it can be argued that the aforementioned data were either anomalous or affected by contaminants. Indeed the laboratory spectra of Reference 4 was later found to be contaminated by HF that was formed in some complex manner from teflon spacers positioned inside the test chamber. In any event the final resolution of this conflict must await spectrally resolved measurements of the atmospheric radiation. Nonetheless it can be of some interest to define alternate atmospheric sources of 2.7 μm radiation that would be consistent with the data base.

Such an analysis has recently been performed² and it was concluded that atmospheric CO₂ is the most likely additional source of 2.7 μm radiation. It is well known that radiation from the CO₂ combination bands (101 \rightarrow 000) and (021 \rightarrow 000) will fall in the 2.7 μm region. These transitions are typically⁵ taken to be 1/25th as weak as the corresponding fundamental band transitions (101, 021 \rightarrow 100, 020). It was pointed out however that if these transitions were only one fourth as weak as the fundamental transition they could prove to be a significant source of 2.7 μm radiation and indeed could provide radiation signatures similar to the anomalous observations discussed above.

The purpose of the present study was to examine, under laboratory conditions, the spectrally resolved fluorescence in the 2.7 μm region occurring in electron irradiated air, and to identify the molecular sources of this radiation. This was done utilizing the AFGL/Optical Physics LABCEDE facility which requires total operating pressures greater than 1 Torr. It must be emphasized that this device does not simulate upper atmospheric conditions. Specifically a high degree of collisional quenching will occur in the test chamber and this quenching can obscure radiative phenomena that might be dominant at the lower pressures of the upper atmosphere.

A description of the test facility and the techniques used in taking the fluorescence data is presented in Section 2. The data analysis and interpretation may be found in Section 3 and summary and conclusions are provided in Section 4.

3. O'Neil, R. R., unpublished results.

4. Murphy, R. E., unpublished results.

5. McClatchey, R. A., Benedict, W. S., Clough, S. A., Burch, D. E., Calfee, R. F., Fox, K., Rothman, L. S., and Garing, J. W. (1973) Atmospheric Absorption Line Parameters Compilation, AFCRL-TR-73-0096.

2. EXPERIMENTAL

The LABCEDE facility is a controlled laboratory apparatus designed to study the fluorescence of electron beam irradiated gas mixtures. In this device a constant pressure, continuously flowing gas is irradiated by a collimated, mono-energetic electron beam. The infrared fluorescence from the irradiated gas target is monitored in a plane perpendicular to the excitation beam. This fluorescence may be both spectrally and temporally resolved through the use of a computer interfaced Michelson interferometer. Because of signal-to-noise limitations, the device cannot be operated at gas pressures below approximately 1 Torr and thus cannot be used to provide an exact simulation of processes occurring in the upper atmosphere, for example, $H \geq 80$ km. In the present studies the observation region flow and pressure conditions, as well as beam current and voltage, were chosen to maximize the fluorescence intensity in the short wavelength infrared (SWIR) near $2.7 \mu\text{m}$.

The LABCEDE apparatus has been described in detail elsewhere,⁶⁻⁹ and only an overview of the facility will be presented here. The electron beam is operated in a pulsed mode and in the present study was characterized by a square-wave pulse of 2.5 msec duration and 25 msec period (10% duty cycle). The electrons are accelerated through an adjustable 32 - 36-kV potential drop, focussed, and sequentially passed through three pinhole nozzles that form a differential pumping network. The differential pumping permits observation chamber operation at pressures of up to 150 Torr while maintaining pressures below 10^{-3} Torr in the electron gun. The electron beam current reaching the observation chamber is largely determined by the amount of beam spreading prior to the last pinhole nozzle. The flow and pressure in the observation region directly affect the nozzle chamber pressure due to pump loading, and thus can affect the amount of beam scattering loss for a given run. Typical electron beam currents were 1 - 2 mA for 32 - 36-kV operation. The beam is maintained at approximately constant operating conditions during the course of a run; short term stability fluctuations and long term drift were both less than 5% of the total current level.

The gases are introduced into the chamber above and to the side of the beam entrance. Mixing of the test gases occurs just outside of the observation chamber.

6. Murphy, R. E., Cook, F. H., Caledonia, G. E., and Green, B. D. (1977) Infrared Fluorescence of Electron Irradiated CO_2 in the Presence of N_2 , Ar and He, AFGL-TR-77-0205.
7. Cook, F. H., and Murphy, R. E. (1976) A Synchronous Signal Processing Technique for Repetitive Arbitrary Waveforms, AFCRL-TR-76-0035.
8. Murphy, R. E., Cook, F. H., and Sakai, H. (1975) Time resolved Fourier spectroscopy, J. Opt. Soc. Amer. 65:600.
9. O'Neil, R., and Davidson, G. (1968) The Fluorescence of Air and Nitrogen Excited by Energetic Electrons, American Science and Engineering, Inc. report ASE-1602 (AFCRL-67-0277).

The gas flow rate is measured with a calibrated flowmeter and accurately controlled by knife-edge needle valves. The chamber pressure is monitored by MKS Baratron capacitance manometer with an atmospheric pressure head, referenced to the electron gun pressure.

The fluorescence is monitored by a lead-salt detector mounted at the exit plane of the scanning Michelson interferometer. The moving interferometer mirror, controlled by a voltage ramp, is continuously scanned. Relative mirror movement is monitored by the interference fringes resulting from a helium-neon laser beam positioned parallel to the fluorescent signal. Constructive interference fringes occur every time the mirror changes position by 0.316 microns. The mirror scanning rate is chosen so that on the average 40 beam pulses occur between laser fringes. The detector signal is bandpass amplified (PARC Model 113), interfaced with a Digital PDP-15 computer using an A/D converter, processed, and stored on magnetic tape.

Observation of the temporal dependence of the fluorescence spectrum is made possible by a sample and hold network referenced to the electron beam pulse onset.⁸ The network output is directly input into the A/D converter, at sampled intervals less than the detection system response time. The A/D converter time resolution limitation is around 40 μ sec, and for these experiments, the resolution limit is determined by the detector and amplification network. Because of the detector limitations it was not possible to measure the emission of the NO fundamental and first overtone vibration/rotation bands simultaneously. A PbSe detector, cooled to 77°K, was used to monitor fluorescence in the mid-wavelength infrared region (MWIR) near 5 μ m. This detector had a 75 μ sec response time which was degraded to 200 μ sec by the bandpass amplifier in order to decrease the noise level. A PbSe detector (at 195°K) was used for the SWIR measurements. This detector exhibits higher responsivity but is limited to a 2 msec response time.

Averaging of the appropriate detector intensities between laser fringes is performed to increase signal-to-noise. These averaged signals are then stored on magnetic tape as a single point in each of the time resolved interferograms. For all the experiments sufficient data points (at different mirror positions) were gathered to provide for 10 cm^{-1} spectral resolution. Degradation of the resolution to artificially decrease the apparent noise level could then be performed mathematically by the computer at a later time if desired.

The gases used in these experiments were ultrahigh purity nitrogen and oxygen, and room air. When use was made of room air, it was introduced into the chamber through the flowmeter and needle valve in order to match the cylinder gas flow conditions as closely as possible. The room air could be filtered to remove dust and water vapor by means of a glass wool/silica gel desiccant trap. This trapping system was found to be effective in removing water vapor from the laboratory air.

The infrared fluorescence intensity was found to be optimized at relatively slow conditions, 2.5 standard liters per min total flow, with pumping of the test chamber occurring only through the electron beam differential pumping system. The optimized chamber operating pressure was 100 Torr and the residence time of the test gas was 30 seconds. Under these flow conditions beam created species are likely to build up in the observation region. Specifically nitrogen and oxygen atoms are produced in the test gas either by direct electron impact dissociations or by subsequent electron/ion/neutral reactions. These atoms can then produce other chemical species such as NO, O₃, NO₂, N₂O. The present experiments are designed to study NO fluorescence resulting from the reactions



If the gas residence time is long compared to the beam pulsing time the amount of NO and other beam created species will increase pulse by pulse until reaching a steady state level. The details of the relevant chemical kinetics for N₂/O₂ mixtures may be found in Reference 6. It is not anticipated that the presence of these beam created species will affect the conclusions of this study however, their presence must be considered when interpreting the experimental observations.

Attempts to decrease the gas residence time result in a loss of fluorescent intensity. Increasing the flow and pumping rates at constant chamber pressure leads to beam current degradation; pressure reduction at constant flow causes a reduction in the total energy deposition of the beam within the field-of-view. As a result, only slow flow measurements were made in the MWIR region. On the other hand, because of the greater sensitivity of the PbS detector, SWIR fluorescence measurements could be made both at the slow flow conditions and also at flow rates of 5 standard liters per minute. For these latter flow rates, and a chamber pressure of 12 Torr, the beam current degradation may be kept at an acceptable level, while the gas chamber residence time is decreased to 2 seconds. Consequently, in these measurements the build-up of beam created species is greatly reduced. Experiments performed in the past⁶ with an integrating sphere in the chamber have resulted in increased signal level at the expense of the residence time and field-of-view definition. No attempt was made to implement the integrating sphere in the present study.

Experimental measurements were first made in the MWIR region in order to observe the temporal behavior of the NO fundamental band radiation ($\Delta v = 1$) with 0.2 msec resolution. Additionally, the presence and relative strengths of radiation from CO₂(ν_3) and N₂O(ν_3) transitions at 4.3 μm and 4.5 μm could be examined.

A series of slow flow runs using first, a mixture of 80% N₂/20% O₂, then trapped (dried) room air, and finally unfiltered room air, were made keeping chamber pressure, beam current, and voltage constant at 100 Torr, 1.6 mA, and 36 kV respectively. When unfiltered air was used, no significant detector signal could be obtained. It is expected that the level of fluorescence in this case is diminished because of the efficient quenching of vibrationally excited states by water vapor.

A similar series of measurements was made in the SWIR, NO overtone, spectral region with the PbS detector. The experimental conditions of the MWIR measurements were duplicated as much as possible. Beam currents achieved were slightly different, 1.2 mA - 1.8 mA, but all other parameters were unchanged. Because of the increased sensitivity of this detector, signal was observed even for the case of unfiltered air. Fast flow measurements were made with both cylinder gases and filtered room air at 36 kV, but at a reduced beam current of 0.9 - 1.4 mA. Although the magnitude of the beam current was decreased in these runs, the current stability was maintained at the 5% fluctuation level. The total fluorescence intensity for these cases was reduced by more than a factor of 2 below that of the slow flow cases.

An additional set of measurements at reduced oxygen partial pressures was made both in the MWIR and SWIR regions. At the same total pressure, it was found that mixtures with fractional oxygen concentrations of $1 - 3 \times 10^{-4}$ of the nitrogen pressure provided the maximum NO fluorescence intensity. The total fluorescence intensity of these runs was a factor of 4 larger than those observed in the air mixtures.

The final collected data base included 8 runs taken with the PbSe detector and 15 runs taken with the PbS detector. In several instances measurements were repeated over a period of several weeks in order to ensure data reproducibility. Furthermore detector spectral response calibrations were performed daily using a black body radiation source. The collected experimental data (stored on magnetic tape) was processed by first sorting the data into time-resolved interferograms, Fourier transforming them into spectra, then applying a correction for detector spectral response and field-of-view. The final form of the reduced data is a series of time-resolved, calibrated spectra for each run. Spectral resolution, up to the maximum of 10 cm^{-1} , is determined by the number of interferogram points included in the transformation. These spectra are then used for species identification and kinetic analysis.

3. DATA ANALYSIS AND INTERPRETATION

The signal-to-noise ratio of the data taken in the MWIR was sufficiently low so that the observed spectra exhibited a "spikey" structure. The apparent noise

level could be diminished by artificially degrading the spectral resolution to 20 cm^{-1} ; however, this had to be done with care inasmuch as real spectral features can be inadvertently washed out by this procedure.

A typical MWIR spectra, taken in a mixture of 80% N_2 /20% O_2 at a total pressure of 100 Torr, is shown in Figure 1. This data was taken with the PbSe detector under slow flow conditions and corresponds to a time just prior to beam termination; the spectral resolution of the data has been degraded to 20 cm^{-1} . Two distinct spectral features are apparent. The first of these, spanning the spectral range of $1760\text{--}1925\text{ cm}^{-1}$, is the result of NO fundamental vibrational/rotational band fluorescence, arising from NO molecules with up to 6 quanta of vibrational excitation. Radiation from the N_2O (ν_3) band is also observed at 2223 cm^{-1} . Note that neither of these species is present in the original test gas and thus both must be created through chemical reactions such as (1) and (2). From a knowledge of the relevant Einstein coefficients,^{5, 10} it can be determined that the populations of the vibrationally excited NO and N_2O responsible for the fluorescence are in the ratio of 7 to 1. No other significant spectral radiators are observed in the bandpass of this detector. (The feature at 1630 cm^{-1} is an artifact of the spectral calibration.)

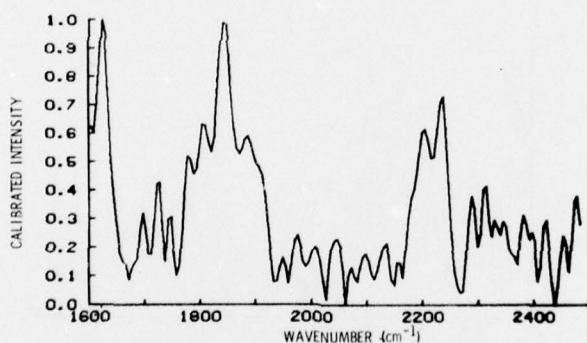


Figure 1. MWIR Fluorescence at Beam Termination From 80% N_2 /20% O_2 Mixtures at 100 Torr Pressure, for Slow-Flow Conditions. Resolution is 20 cm^{-1} . Electron beam current was 1.6 mA, voltage was 36 kV. NO and N_2O (ν_3) radiation are evident

The same spectrum is shown in Figure 2 at 10 cm^{-1} resolution. The large noise level is due to the combination of poor detector response and low fluorescence levels. It can be seen, however, that the basic spectral features of Figures 1 and 2

10. Billingsley, II, F.P. (1976) Calculated vibration rotation intensities for $\text{NO}(X^2\Pi)$, *J. Molec. Spectrosc.* 61:53.

are the same. The spectrum of Figure 3 corresponds to the same case at a time of 0.2 msec after beam termination. The time difference between Figures 2 and 3 is equal to the response time of the detection network. The intensity scale is the same for both figures and it can be seen that with increased time the fluorescence due to NO is greatly diminished, while the N_2O signal is essentially unchanged. The rate constants for vibrational quenching of NO ($v=1$) by N_2 and O_2 have been measured¹¹ as 1.7×10^{-16} cm³/sec and 2.4×10^{-14} cm³/sec respectively leading to a predicted NO fluorescence decay time of 0.07 msec for the present case. The observed NO decay is limited by the time resolution of the experiment. $N_2O(\nu_3)$ quenching by N_2 has been measured¹² to have a rate constant of 4×10^{-15} cm³/sec, and thus the $N_2O(\nu_3)$ fluorescence would be expected to decay on the same time scale, as NO, 10^{-4} seconds. The N_2O fluorescence in this experiment is observed to decay with a time constant of 20 msec, thus implying the presence of a source of N_2O vibrational excitation in the test gas after beam termination. Vibrationally excited molecular nitrogen (that is, excited by beam electrons) is a known energy reservoir under these conditions⁶ and near-resonance vibrational exchange between $N_2O(\nu_3)$ and $N_2(v)$ is postulated as an explanation for the observed slow N_2O decay.

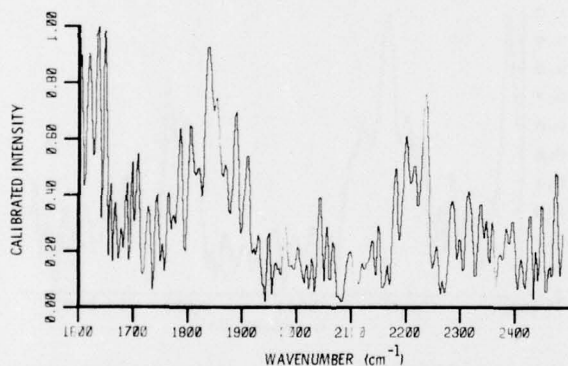


Figure 2. MWIR Fluorescence of Figure 1 at Beam Termination With 10 cm^{-1} Resolution. Normalized to $I_{\text{max}} = 6.9 \times 10^{-9} \text{ W/cm}^2\text{-str-cm}^{-1}$

11. Murphy, R.E., Lee, E.T.P., and Hart, A.M. (1975) Quenching of vibrationally excited nitric oxide by molecular oxygen and nitrogen, *J. Chem. Phys.* **63**:2919.
12. Yardley, J.T. (1968) Vibration-to-vibration energy transfer in gas mixtures containing nitrous oxide, *J. Chem. Phys.* **49**:2816.

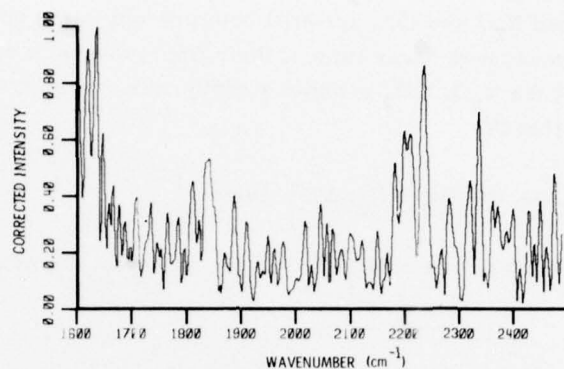
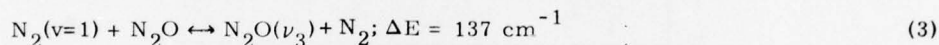


Figure 3. MWIR Fluorescence 0.2 msec After Beam Termination for the Same Run as Figure 2. Resolution is 10 cm^{-1} . Maximum intensity is $6.9 \times 10^{-9} \text{ W/cm}^2\text{-str-cm}^{-1}$

Specifically, the vibrational exchange reaction



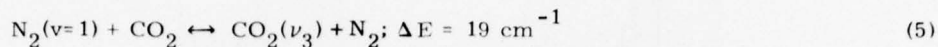
is assumed to be in local steady state so that to first order

$$\frac{\text{N}_2(v=1)}{\text{N}_2} = \frac{\text{N}_2\text{O}(\nu_3)}{\text{N}_2\text{O}} e^{-\Delta E/kT} \quad (4)$$

and thus, since N_2O is a trace species, the decay of $\text{N}_2\text{O}(\nu_3)$ mirrors the decay of vibrationally excited N_2 . The large energy defect between N_2 and NO , 484 cm^{-1} , precludes a similar effect in the case of NO .

In Figure 4 the spectrum of irradiated filtered room air under slow-flow conditions is displayed at beam termination. Both NO and $\text{N}_2\text{O}(\nu_3)$ fluorescence are observed along with radiation from $\text{CO}_2(\nu_3)$ at 2350 cm^{-1} ($4.3 \text{ }\mu\text{m}$) as expected. The $\text{N}_2\text{O}(\nu_3)$ fluorescence intensity is increased by 20% over that of the N_2/O_2 runs of Figures 2 and 3, while the NO fluorescence has decreased by a third. Carbon dioxide is the dominant spectral radiator. From consideration of the relative bandstrengths of CO_2 , N_2O , and NO , it may be estimated that the $\text{N}_2\text{O}(\nu_3)$ and $\text{NO}(v)$ concentrations at beam termination relative to that of $\text{CO}_2(\nu_3)$ are 1.4 and 5.6 to 1 respectively. A spectrum from the same case corresponding to the fluorescence 0.2 msec after beam termination is shown in Figure 5. Again the NO fluorescence has disappeared while both the N_2O and CO_2 fluorescence remain unchanged. The fluorescence detected 3.4 msec after beam termination is displayed in Figure 6.

Vibrationally excited N_2O and CO_2 are still both present in the same relative concentrations. The measured decay time of their fluorescence is approximately 14 milliseconds. Like N_2O , CO_2 exhibits a rapid near resonant vibrational exchange reaction with N_2 , that is,



and thus the CO_2 fluorescence will also mirror the decay of vibrationally excited N_2 .

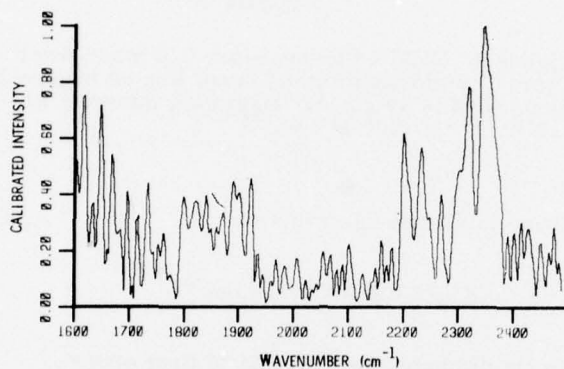


Figure 4. MWIR Fluorescence at Beam Termination From Filtered Room Air at 100 Torr Pressure and Slow-Flow Conditions. Resolution is 10 cm^{-1} , $i = 1.6 \text{ mA}$. Radiation from NO , $N_2O(\nu_3)$ and $CO_2(\nu_3)$ can be observed. Maximum intensity is $1.1 \times 10^{-8} \text{ W/cm}^2\text{-str-cm}^{-1}$

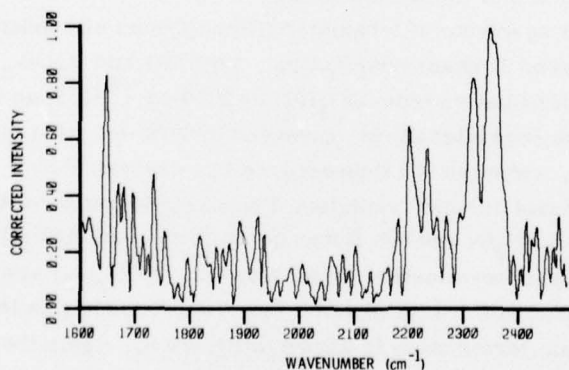


Figure 5. Fluorescence 0.2 msec After Beam Termination for Conditions of Figure 4. Maximum intensity is $1.1 \times 10^{-8} \text{ W/cm}^2\text{-str-cm}^{-1}$

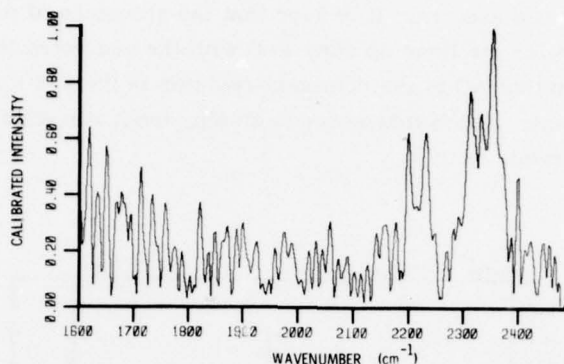


Figure 6. Fluorescence at 3.4 msec After Beam Termination for Run of Figures 4 and 5. $\text{CO}_2(\nu_3)$ and $\text{N}_2\text{O}(\nu_3)$ Radiation are only slightly diminished from beam termination values. Maximum intensity is $9.1 \times 10^{-9} \text{ W/cm}^2\text{-str-cm}^{-1}$

A spectrum taken under slow-flow conditions in filtered room air using the PbS detector is shown in Figure 7. This spectrum, corresponding to the time of beam termination, has a resolution of 20 cm^{-1} and is uncorrected for the spectral response of the detector; the $\text{CO}_2(\nu_3)$ radiation at 2350 cm^{-1} is by far the strongest feature observed although this detector is relatively insensitive to $4.3 \mu\text{m}$ radiation. $\text{N}_2\text{O}(\nu_3)$ fluorescence, not a prominent feature in the spectrum shown, has also been observed with the PbS detector. The calibrated intensity of the $\text{CO}_2(\nu_3)$ radiation shown in Figure 7 agrees to within 20% with a value obtained using the PbSe detector under similar experimental conditions. This excellent agreement reflects both the accuracies of the detector calibrations and the good run-to-run reproducibility of the data base. The other spectral features evident in Figure 7 are the radiation of interest in the spectral range of $3500 - 3800 \text{ cm}^{-1}$ and the sharp features around 5500 cm^{-1} ($1.8 \mu\text{m}$) which have been identified as atomic oxygen and nitrogen lines in previous studies performed at the Air Force Geophysics Laboratory.¹³

Figure 8 displays a calibrated version of the spectrum of Figure 7 over the spectral range of $3100 - 3800 \text{ cm}^{-1}$ ($3.23 - 2.63 \mu\text{m}$). Also shown for comparison is a computer generated NO first overtone spectrum. The generated spectrum is calculated using the latest spectroscopic constants of NO and includes contributions from both total angular momentum states. The shapes of all vibrational/rotation transitions in the synthetic spectrum are broadened by a sinc slit function appropriate to the interferometer used in the experiments. The synthesized spectrum

13. Murphy, R. E., Fairbarn, A. R., Rogers, J. W., and Hart, A. M. (1975) Near IR Nuclear Spectra: Interpretation by Recent Laboratory Results, presented at the Fourth Strategic Space Symposium, Monterey, CA.

was chosen to have a Boltzmann vibrational distribution corresponding to a vibrational temperature of 5000°K and a rotational temperature of 300°K; no attempt has been made to fit the two spectra. It is seen that the structure of the experimental spectrum taken in room air lines up very well with the predicted NO spectrum, leading to the conclusion that NO is the dominant radiator in the 2.6 - 3.2 μm region under these conditions. Again fluorescence arising from vibrational excited NO up to level $v=6$ is observed.

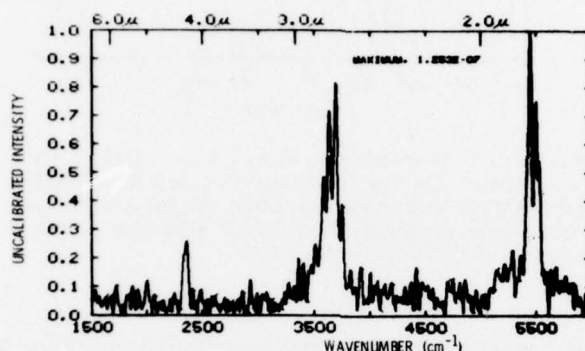


Figure 7. Uncalibrated Fluorescence Observed With PbS Detector at Beam Termination From Filtered Room Air Under Standard Slow-Flow Conditions. Resolution is 20 cm^{-1} . Radiation observed is from $\text{CO}_2(\nu_3)$ at 4.3 μm , $\text{NO}(\Delta v=2)$ at 2.7 μm and atomic O and N at 1.8 μm

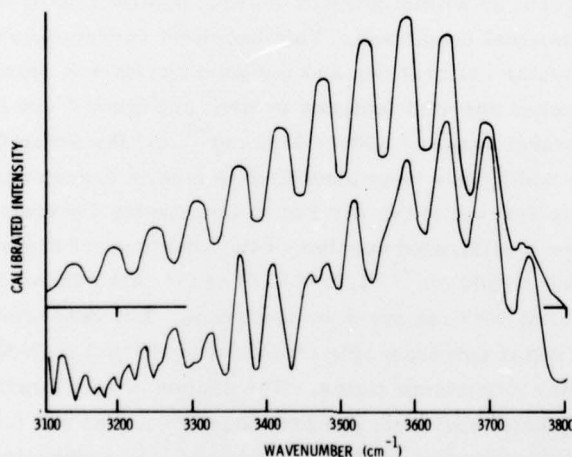


Figure 8. Comparison of SWIR Fluorescence with Synthetic Spectrum of NO
Lower trace: Expansion of 3100 - 3800 cm^{-1} Region of Figure 7. Calibrated maximum intensity is $1.5 \times 10^{-10} \text{ W/cm}^2\text{-sr-cm}^{-1}$. Upper trace: Synthesized spectrum of NO overtone radiation (see text for details)

When the spectral resolution is increased to 10 cm^{-1} reproducible features not attributable to NO appear, as is shown in Figure 9. Although the noise level of the 10 cm^{-1} calibrated spectrum is greater than the 20 cm^{-1} spectrum of Figure 8, the features indicated by arrows are reproducible both as a function of time and from run to run. The expected spectral shapes of the $\text{N}_2\text{O}(02^{\circ}1 \rightarrow 00^{\circ}0)$ and $(10^{\circ}1 \rightarrow 00^{\circ}0)$ combination bands as well as the $\text{CO}_2(02^{\circ}1 \rightarrow 00^{\circ}0)$ and $(10^{\circ}1 \rightarrow 00^{\circ}0)$ combination bands are also shown in Figure 9. It is clear that CO_2 radiation does not occur in any significant amount in this spectral region. The N_2O combination band at 3480 cm^{-1} does seem to match the frequency, if not the shape, of some of the unidentified spectral features. (This band is predicted to be the strongest in this spectral region⁵ for N_2O in vibrational equilibrium at room temperature.) Nonetheless, even if the 3480 cm^{-1} features are attributed to N_2O , other strong features remain unexplained.

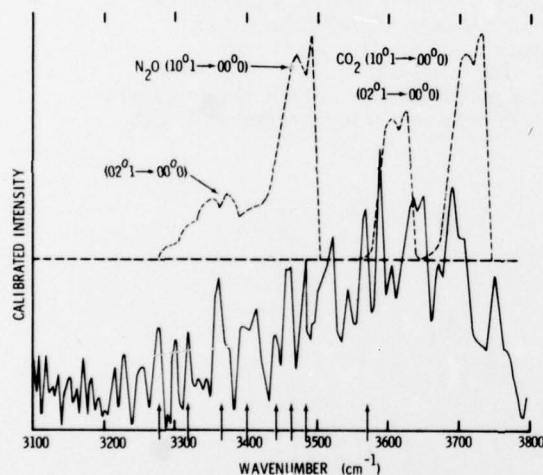


Figure 9. Spectrum of Filtered Room Air with Estimated CO_2 and N_2O Bands Shown for Comparison. Lower trace: spectrum of filtered room air is as in Figures 6 and 7 at 10 cm^{-1} resolution. Maximum calibrated intensity is $1.8 \times 10^{-10}\text{ W/cm}^2\text{-str-cm}^{-1}$. Upper trace: estimated N_2O and CO_2 combination band shapes and relative intensities. Arrows along bottom axis indicate reproducible features not due to NO

The SWIR spectrum of a slow-flow run taken with a 80% N_2 /20% O_2 mixture is shown in Figure 10. The data, shown with 10 cm^{-1} resolution, is taken at the time of beam termination. Again, as for the filtered room air cases, NO is the dominant radiator in the spectral region shown. The lack of significant CO_2 radiation in this spectral region is demonstrated in Figure 11 which provides a comparison between the spectra recorded in filtered room air and an 80% N_2 /20% O_2 mixture where no CO_2 should be present. It can be seen that there are no observable differences between the two scans with the exception that the laboratory-air case appears to have a somewhat greater spectral resolution. Interestingly enough even the features

attributed to noise appear to line up; the unexplained spectral features of the air runs are also present in the N_2/O_2 experiments.

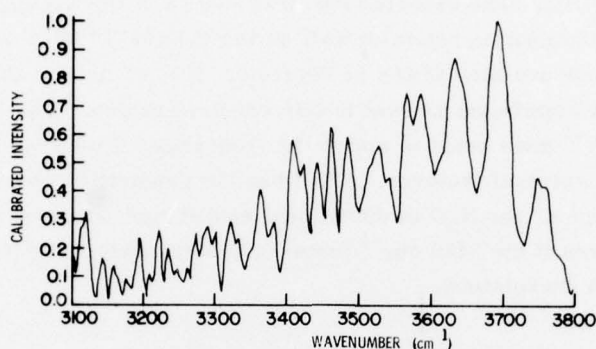


Figure 10. SWIR Fluorescence From 80% $N_2/20\%O_2$ Mixtures at 100 Torr Pressure Under Slow-Flow Conditions. Resolution is 10 cm^{-1} . Maximum intensity is $3.6 \times 10^{-10} \text{ W/cm}^2\text{-str-cm}^{-1}$. Increase in NO radiation is in agreement with MWIR observations — NO fluorescence was decreased in the presence of CO_2

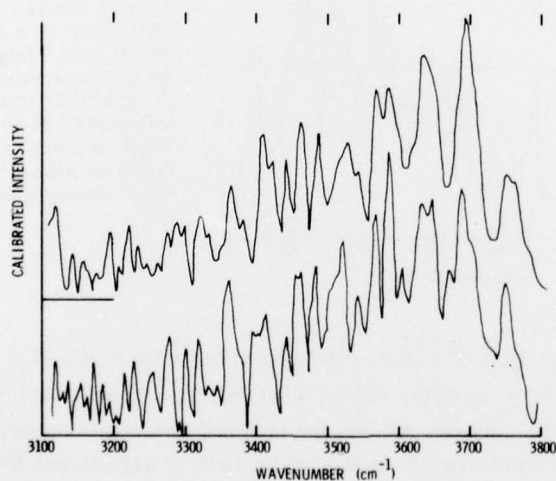


Figure 11. Comparison of N_2/O_2 and Room Air Spectra Taken Under Similar Conditions. Resolution is 10 cm^{-1} . Lower trace: room air fluorescence (Figure 9). Upper trace: N_2/O_2 fluorescence (Figure 10)

Measurements taken under faster flow conditions and for much shorter residence times yield similar spectra. In these cases only runs using the PbS detector were possible due to decreased signal intensity, but the unidentified features remained. If these features were attributable to a build up of beam created species, such as N_2O , their relative intensity should have been greatly diminished because of the decreased residence time. In fact, $N_2O(\nu_3)$ radiation at $4.5 \mu m$ was no longer observed for these runs (with the PbS detector). Radiation arising from $NO \Delta v=2$ transitions is still the dominant radiation source at $2.7 \mu m$ under these conditions, and the NO vibrational distribution appears to be very similar to that of the higher pressure runs.

The experiments performed using trace concentrations of oxygen mixed with nitrogen provided slightly more signal in the MWIR region. No evidence of N_2O fluorescence at $4.5 \mu m$ is observed in these spectra. The observed vibrational distribution of NO is not greatly different from that of the 80% N_2 /20% O_2 mixture data of Figure 2. In these runs the nitrogen pressure was varied from 25 - 115 Torr and the oxygen pressure, set to achieve maximum intensity, was varied from 0.2 - 0.75 Torr. No variation in the observed NO excited vibrational distribution was noted over this range of conditions. The measured NO fluorescence decay rate was in good agreement with previous observations.¹¹ A more systematic study of this type might permit the measurement of individual vibrational level decay rates of NO by N_2 and O_2 .

When the PbS, SWIR sensitive detector was used, the observed NO spectral intensity increased by a factor of 2 over the air cases. The unidentified features noted previously all increased by an even greater amount, about a factor of 4, and are the most prominent spectral features, as shown in Figure 12. The displayed spectrum is from a 100-Torr N_2 , 0.03-Torr O_2 slow-flow run, and corresponds to the time of beam termination. The NO vibrational bands are greatly obscured by the sharp spiked features that have widths equal to the experimental resolution. Since unresolved vibration-rotational bands would have spectral widths much greater than this, the features were suspected to be either due to atomic lines or individual rotational lines of a molecular vibrational band.

Under certain conditions the unidentified spectral features were found to persist long after NO fluorescence had decayed. Figure 13 shows a spectrum taken in the same experiment as Figure 12, but at a time corresponding to 3.4 msec after beam termination. Some residual NO radiation from the slowest decaying observable level ($v=2$) might be present between 3650 and 3770 cm^{-1} . Most striking, however, is the appearance of the unidentified spectral features. Indeed some weaker features attributed to noise in the other runs are observed to be reproducible with time under these conditions. Note that the relative intensity of the lines appears unchanged from early time observations, see comparison of Figures 12 and 13. These long

time observations provided a much clearer picture of the unidentified radiator. Specifically the strong feature at $\sim 3560 \text{ cm}^{-1}$ was noted to agree well with the frequency of the Q branch of the $\text{OH}(v=1 \rightarrow 0)$ transition. The free radical OH was considered a likely radiation source inasmuch as water was introduced into the system with the room air and could have a long residence time on the chamber surfaces for typical system pumping rates.

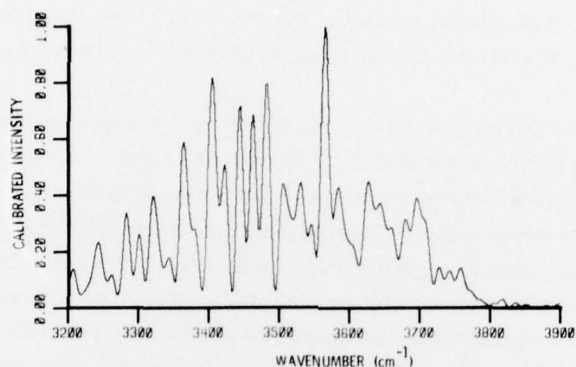


Figure 12. SWIR Fluorescence From a Trace Oxygen Run Under Slow-Flow Conditions. The N_2 pressure is 100 Torr. O_2 pressure is 0.03 Torr. Resolution is 10 cm^{-1} and maximum intensity is $6.1 \times 10^{-10} \text{ W/cm}^2\text{-str-cm}^{-1}$ at beam termination. The NO radiation is no longer the dominant spectral radiation

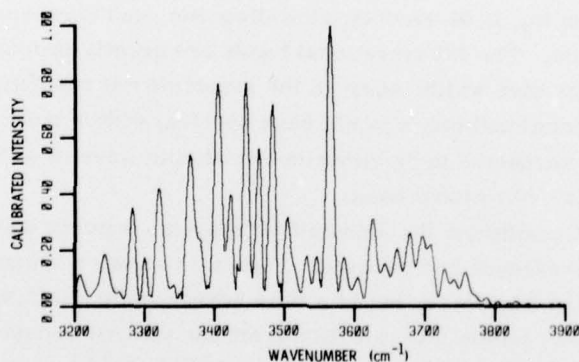


Figure 13. SWIR Fluorescence 3.5 msec After Beam Termination for Run of Figure 12. Maximum intensity is $1.9 \times 10^{-10} \text{ W/cm}^2\text{-str-cm}^{-1}$. The NO overtone radiation has virtually disappeared, isolating the spectral lines of interest

In order to verify the tentative assignment, a synthetic spectrum of the OH molecule was generated. The OH free radical has an inverted $^2\Pi$ ground electronic state with strong coupling between spin and angular momentum giving rise to two total angular momentum manifolds of states $\Omega=1/2$ and $3/2$. Transitions between similar states within these manifolds are not degenerate and should be easily observable. Coupling of rotation to the total angular momentum is a complex function of the rotational and vibrational energy and a vibrating rotor-anharmonic oscillator model of the spectrum is not sufficient. Detailed predictions of the OH spectral line positions and strengths have been performed by Mies¹⁴ and shown to be in good agreement with experimental spectra. Mies' calculated frequencies and Einstein coefficients were used to generate a synthetic OH spectrum using a sinc slit function and assuming a 300°K rotational temperature. A comparison between this synthesized spectrum and the long time spectrum of Figure 13 is presented in Figure 14.

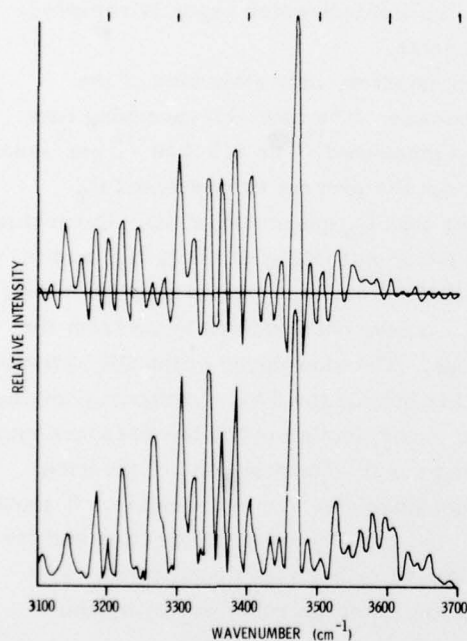


Figure 14. Comparison of Synthetic Spectrum of OH With Spectral Features of Figure 13. All significant features (except 3270 cm^{-1} line) are matched by OH predictions

(Note that the synthetic spectrum exhibits negative values of intensity. This is a result of convoluting the predicted OH spectrum over a sinc slit function which displays prominent negative sidelobes. This effect is an artifact of the Fourier

14. Mies, F. H. (1974) Calculated vibrational transition probabilities of $\text{OH}(X^2\Pi)$, *J. Molec. Spectrosc.* 53:150.

transform.) It can be seen that the prominent spectral features match OH vibration/rotation lines. In addition, excellent agreement occurs between the spectral positions of nearly all of the weaker features and OH lines arising from high J levels and the weaker, $\Omega_{1/2}$ transitions. Note that in the synthetic spectrum, the relative populations of the two spin states and the rotational levels are assumed to be in the thermal equilibrium with the gas kinetic temperature. The observed relative OH vibrational populations can be readily determined from the measured Q branch intensities and it has found that the relative populations of OH $v=2$ and $v=1$ are nearly equal at beam termination ($n_2/n_1=0.8$) for all the runs in which they could be observed (including trace oxygen, and fast and slow-flow cylinder gas and room air runs.)

Upon backchecking it was found that the OH spectrum was not observed in early runs made using cylinder gases prior to that admission of room air into the chamber. Thus it appears that once water vapor was admitted it strongly adhered to the chamber surfaces and ultimately gave rise to the OH fundamental band radiation even in "dry" air mixtures. Additionally, not all the ambient water vapor is removed by the trap in the filtered room air measurements.

Due to the slow time response of the PbS detector, only estimates of the quenching rates of OH by O_2 and N_2 could be made. The total OH quenching rate constant by an air mixture of N_2/O_2 has been measured¹⁵ as 1.5×10^{-14} cm³/sec, dominated by O_2 quenching. Observations from the present work support O_2 quenching of OH as faster than N_2 , but slower than O_2 quenching of NO. Quenching of OH by N_2 appears to be significantly faster than quenching of NO by N_2 , and is estimated to have a rate constant of order 1.5×10^{-15} cm³/sec which is approximately 10% of the rate constant for quenching by O_2 . These observations arise from the analysis of the low pressure trace oxygen runs. The slow decay of the OH radiation in Figures 12 and 13 ($P=100$ Torr) can possibly be explained by vibrational pumping from $N_2(v \geq 2)$ which would not make as large a contribution in the low pressure runs (a more detailed investigation is obviously required). Observations of the decay OH($v=2$) are limited and estimates of the quenching rates are not possible. It should be emphasized that the present study was not designed to study OH kinetics and the above observations must be considered qualitative rather than quantitative. For example the possible chemical destruction of OH, through reactions with beam produced species, has not been considered.

15. Murphy, R.E. (1971) Infrared emission of OH in the fundamental and first overtone bands, J. Chem. Phys. 54:4852.

4. SUMMARY AND CONCLUSIONS

In summary, an examination of the infrared fluorescence arising from both electron irradiated air and nitrogen/oxygen mixtures has been provided. The study was limited to the spectral range of $1600 - 6700 \text{ cm}^{-1}$ ($1.5 - 6 \text{ }\mu\text{m}$) by detector response/system background considerations. The dominant spectral features observed included fluorescence from: (a) previously identified atomic nitrogen and oxygen transitions occurring near 5500 cm^{-1} , (b) the fundamental and first overtone vibrational bands of NO, and (c) the fundamental bands of the ν_3 modes of CO_2 and N_2O . The CO_2 fluorescence was of course not observed in irradiated mixtures of bottled N_2/O_2 , but rather only when room air was admitted into the test chamber. Lastly a persistent contaminant radiator, observed in the majority of the measurements, has been identified as OH.

The basic conclusion of this report is that, for the conditions considered, there is no evidence of CO_2 combination band radiation occurring at or near $2.7 \text{ }\mu\text{m}$ in electron irradiated air. This is true even though non-equilibrium concentrations of $\text{CO}_2(\nu_3)$ were observed. Indeed, in the $2.7 \text{ }\mu\text{m}$ region, there are no significant differences between the spectra observed in air and in 80% N_2 /20% O_2 mixtures. These results are specific to pressures of 10 - 100 Torr and need not be representative of upper atmospheric phenomena. This is because the level of CO_2 combination band fluorescence is proportional to the populations of the $\text{CO}_2 \nu_1$ and ν_2 modes which in turn can be controlled by the rate of vibrational quenching collisions which is altitude dependent.

A number of interesting side features that could be studied in more detail have been observed in this data. These include: (a) the observation of OH fluorescence and decay which might be utilized to ascertain fundamental quenching rate constants for vibrationally excited OH, (b) NO fluorescence data sufficiently resolved to allow determination of vibrational level dependent quenching rate constants and relative fundamental to first overtone band Einstein coefficients, and (c) the possibility of using trace quantities of CO_2 to determine relative populations of N_2O and vibrationally excited N_2 .

References

1. Proceedings of the HAES Infrared Data Review, 13-15 June 1977, Falmouth, MA, AFGL Report OP-TM-05.
2. Proceedings of the HAES Infrared Data Review, 13-15 June 1977, AFGL Report OP-TM-05, pp 327-341, presented by H. Mitchell.
3. O'Neil, R.R., unpublished results.
4. Murphy, R.E., unpublished results.
5. McClatchey, R.A., Benedict, W.S., Clough, S.A., Burch, D.E., Calfee, R.F., Fox, K., Rothman, L.S., and Garing, J.S. (1973) Atmospheric Absorption Line Parameters Compilation, AFCRL-TR-73-0096.
6. Murphy, R.E., Cook, F.H., Caledonia, G.E., and Green, B.D. (1977) Infrared Fluorescence of Electron Irradiated CO₂ in the Presence of N₂, Ar and He, AFGL-TR-77-0205.
7. Cook, F.H., and Murphy, R.E. (1976) A Synchronous Signal Processing Technique for Repetitive Arbitrary Waveforms, AFCRL-TR-76-0035.
8. Murphy, R.E., Cook, F.H., and Sakai, H. (1975) Time resolved Fourier spectroscopy, J. Opt. Soc. Amer. 65:600.
9. O'Neil, R., and Davidson, G. (1968) The Fluorescence of Air and Nitrogen Excited by Energetic Electrons, American Science and Engineering, Inc. report ASE-1602 (AFCRL-67-0277).
10. Billingsley, II, F.P. (1976) Calculated vibration rotation intensities for NO(X²II), J. Molec. Spectrosc. 61:53.
11. Murphy, R.E., Lee, E.T.P., and Hart, A.M. (1975) Quenching of vibrationally excited nitric oxide by molecular oxygen and nitrogen, J. Chem. Phys. 63:2919.
12. Yardley, J.T. (1968) Vibration-to-vibration energy transfer in gas mixtures containing nitrous oxide, J. Chem. Phys. 49:2816.
13. Murphy, R.E., Fairbarn, A.R., Rogers, J.W., and Hart, A.M. (1975) Near IR Nuclear Spectra: Interpretation by Recent Laboratory Results, presented at the Fourth Strategic Space Symposium, Monterey, CA.
14. Mies, F.H. (1974) Calculated vibrational transition probabilities of OH(X²II), J. Molec. Spectrosc. 53:150.
15. Murphy, R.E. (1971) Infrared emission of OH in the fundamental and first overtone bands, J. Chem. Phys. 54:4852.

DNA DISTRIBUTION LIST

DEFENSE ADVANCED RSCH PROJ AGENCY

LTC W. A. WHITAKER
STO
MAJ GREGORY CANAVAN

DEFENSE DOCUMENTATION CENTER TC

DEFENSE NUCLEAR AGENCY
RAAE CHARLES A. BLANK
TITL TECH LIBRARY
TISI ARCHIVES
RAEV HAROLD FITZ, JR.
RAAE MAJ J. MAYO
RAAE G. SOPER
MAJ R. BIGONI

DIR OF DEFENSE RSCH &
ENGINEERING
DEPARTMENT OF DEFENSE
DD/S&SS DANIEL BROCKWAY
DD/S&SS(OS)

FIELD COMMAND
DEFENSE NUCLEAR AGENCY
FCRP

LIVERMORE DIVISION FLD
COMMAND DNA
FCPRL

ATMOSPHERIC SCIENCES
LABORATORY
DRSEL-BL-SY-A F. NILES
H. BALLARD

HARRY DIAMOND LABORATORIES
DRXDO-NP F. H. WIMINETZ

U.S. ARMY NUCLEAR AGENCY
MONA-WE

BMD ADVANCED TECH CTR
ATC-O, W. DAVIES
ATC-T, M. CAPPS

DEP. CHIEF OF STAFF FOR RSCH
DEV & ACQ

DEPARTMENT OF THE ARMY
MCB DIVISION
DAMA-CSZ-C

U.S. ARMY BALLISTIC RESEARCH LABS

DRXBR-AM, G. KELLER
DRXRD-BSP, J. HEIMERL
JOHN MESTER
TECH LIBRARY

US ARMY ELECTRONICS COMMAND
INST FOR EXPL RSCH
DRSEL
STANLEY KRONENBERGER
WEAPONS EFFECTS SECTION

US ARMY FOREIGN SCIENCE &
TECH CTR
ROBERT JONES

US ARMY RESEARCH OFFICE
ROBERT MACE

NAVAL OCEANS SYSTEMS CENTER
CODE 2200 ILAN ROTHMULLER
CODE 2200 HERBERT HUGHES
CODE 2200 JURGEN RICHTER
CODE 2200-WILLIAM MOLER
CODE 2200 RICHARD PAPPERT

NAVAL RESEARCH LABORATORY
CODE 7712 DOUGLAS P. MCNUTT
CODE 7701 JACK D. BROWN
CODE 2600 TECH LIB
CODE 7237 CHARLES Y. JOHNSON
CODE 7700 TIMOTHY P. COFFEY
CODE 7709 WAHAB ALI
CODE 7750 DARRELL F. STROBEL
CODE 7750 PAUL OULUENNE
CODE 7750 J. FEDDER
CODE 7750 S. OSSAKON
CODE 7750 J. DAVIS

NAVAL SURFACE WEAPONS CENTER
CODE WA501 NAVY NUC
PRGMS OFF
TECHNICAL LIBRARY

SUPERINTENDENT
NAVAL POST GRADUATE SCHOOL
TECH REPORTS LIBRARIAN

NAVAL ELECTRONICS SYSTEMS
COMMAND
PME 117

NAVAL INTELLIGENCE SUPPORT CNTR
DOCUMENT CONTROL

AF GEOPHYSICS LABORATORY, AFCS
LKB KENNETHS. W. CHAMPION
OPR ALVA T. STAIR, Jr
OPR-1 J. ULWICK
OPR-1 R. MURPHY
OPR-1 J. KENNEALY
PHG J.C. MCCLAY
LKD ROCCO NARCIS
LKO R. HUFFMAN

AF WEAPONS LABORATORY AFSC
SUL
MAJ GARRY GANONG, DYM

COMMANDER
ASD
ASD-YH-EX LTC
ROBERT LEVERETTE

SAMSO/AW
SZJ MAJ LAWRENCE DOAN
AWN

AFTAC
TECH LIBRARY
TD

HQ
AIR FORCE SYSTEMS COMMAND
DLS
TECH LIBRARY
DLCAW
DLTW
DLXP
SDR

HQ USAF/RD
RDQ

ROME AIR DEVELOPMENT CTR
J.J. SIMONS OCSC

DIVISION OF MILITARY
APPLICATION
DOC CON

LOS ALAMOS SCIENTIFIC
LABORATORY
DOC CON FOR R. A. JEFFERIES
DOC CON FOR C. R. MEHL
ORG 5230
DOC CON FOR H. V. ARGO
DOC CON FOR M. TIERNEY
J-10
DOC CON FOR
ROBERT BROWNLEE
DOC CON FOR WILLIAM MAIER
DOC CON FOR JOHN ZINNY
DOC CON FOR REFERENCE
LIBRARY ANN BEYER

SANDIA LABORATORIES -
LIVERMORE, CA
DOC CONTROL FOR
THOMAS COOK ORG 8000

SANDIA LABORATORIES -
ALBUQUERQUE, NM
DOC CON FOR W. D. BROWN
ORG 1353
DOC CON FOR L. ANDERSON
ORG 1247
DOC CON FOR MORGAN KRAMMA
ORG 5720
DOC CON FOR FRANK HUDSON
ORG 1722
DOC CON FOR SANDIA REPTS
COLL. ORG 3422-1

ARGONNE NATIONAL LABORATORY
DOC CON FOR A. C. WAHL
DOC CON FOR DAVID H. GREEN
DOC CON FOR LIB SVCS RPTS
SEC
DOC CON FOR S. GABELNICK
DOC CON FOR GERALD T. REEDY

UNIVERSITY OF CALIFORNIA
W. H. DUEWER GEN L-404
JULIUS CHANG L-71
G. R. HAUGEN L-404
D. J. WUERBLES L-142

US ENERGY RSCH & DEV ADMIN
DOC CON FOR CLASS TECH LIB

DEPARTMENT OF TRANSPORTATION
SAMUEL C. CORONITI

NASA
GODDARD SPACE FLIGHT CENTER
A. C. AIKEN
A. TEMPKIN
J. BAUER
TECHNICAL LIBRARY
J. SIRY

NASA
A. GESSOW
D. P. CAUFFMAN
LTC D. R. HALLENBECK CODE SG
R. FELLOWS
A. SCHARDT
M. TEPPER

NASA
LANGLEY RSCH CENTER
CHARLES SCHEXNAYDER MS-16A

NASA
AMES RSCH CENTER
N-254-4 WALTER L. STARR
N-254-4 R. WHITTEN
UNCL ONLY
N-254-4 ILIA G. POPPOFF
N-254-3 NEIL H. FARLOW

NASA
GEORGE C. MARSHALL SPACE
FLIGHT CENTER
C.R. BALCHER
N.H. STONE
CODE ES22 JOHN WATTA
W.T. ROBERTS
R.D. HUDSON
R. CHAPPELL

ALBANY METALLURGY RSCH CTR
ELEANOR ARSHIRE

CENTRAL INTELLIGENCE AGENCY
NES/OSI - 2G48 HQS

DEPARTMENT OF COMMERCE
SEC OFFICER FOR
JAMES DEVOR
SEC OFFICER FOR
STANLEY ABRAMOWITZ
SEC OFFICER FOR
J. COOPER
SEC OFFICER FOR
GEORGE A. SINNATT
SEC OFFICER FOR
K. KESSLER
SEC OFFICER FOR
M. KRAUSS
SEC OFFICER FOR
LEWIS H. GEVANTMAN
SEC OFFICER FOR
JAMES DEVCE

NATIONAL OCEANIC &
ATMOSPHERIC ADMIN
GEORGE C. REID
AERONOMY LAB
UNCL ONLY
ELDON FERGUSON
FRED FEHSENFELD

AERO-CHEM RSCH
LABORATORIES INC.
A. FONTIJN
H. PERGAMENT

AERODYNE RESEARCH, INC.
F. BIEN
M. CAMAC

AERONOMY CORPORATION
S.A. BOWHILL

AEROSPACE CORPORATION
N. COHEN
HARRIS MAYER
SIDNEY W. KASH
T. WIDHOPH
R.J. MCNEAL
R. GROVE
IRVING M. GARFUNKEL
THOMAS D. TAYLOR
V. JOSEPHSON
JULIAN REINHEIMER
R.D. RAWCLIFFE

AVCO-EVERETT RSCH
LABORATORY, INC.
TECHNICAL LIBRARY
GEORGE SUTTON
C.W. VON ROSENBERG, JT

BATTELLE MEMORIAL INSTITUTE
DONALD J. HAMMAN
STOIAIC
RICHARD K. THATCHER

THE TRUSTEES OF BOSTON COLLEGE
CHAIRMAN DEPT OF CHEM

BROWN ENGINEERING COMPANY, INC.
N. PASSINO
RONALD PATRICK

CALIFORNIA AT RIVERSIDE, UNIV OF
ALAN C. LLOYD
JAMES N. PITTS, JR.

CALIFORNIA AT SAN DIEGO, UNIV OF
S.C. LIN

CALIFORNIA INSTITUTE OF
TECHNOLOGY
JOSEPH AJELLO

CALIFORNIA, UNIVERSITY OF
SEC OFFICER FOR
HAROLD JOHNSTON
SEC OFFICER FOR
F. MOZER
SEC OFFICER FOR
DEPT OF CHEM W. MILLER

CALIFORNIA, STATE OF
LEO ZAFONTE

CALSPAN CORPORATION
C. E. TREANOR
G. C. VALLEY
M. G. DUNN
W. WURSTER

COLORADO, UNIVERSITY OF
A. PHELPS JILA
JEFFREY B. PEARCE LASP
C. BEATY JILA
C. LINEBERGER JILA
CHARLES A. BARTH LASP

COLUMBIA UNIVERSITY, THE
TRUSTEES OF
RICHARD ZARE
SEC OFFICER H. M. FOLEY

CONCORD SCIENCES
EMMETT SUTTON

DENVER, UNIVERSITY OF
SEC OFFICER FOR VAN ZYL
SEC OFFICER FOR
DAVID MURCRAY

GENERAL ELECTRIC COMPANY-
TEMPO CENTER FOR
ADVANCED STUDIES
DASAIC
WARREN S. KNAPP
TIM STEPHEN
DON CHANDLER
B. CAMBILL

GENERAL ELECTRIC COMPANY-
SPACE DIVISION-
VALLEY FORGE SPACE CTR
M. H. BORTNER -
SPACE SCIENCE LAB
J. BURNS
F. ALYEA
P. ZAVITSANDS
R. H. EDSALL
T. BAURER

GENERAL RSCH CORPORATION
JOHN ISE, Jr.

GEOPHYSICAL INSTITUTE
D. J. HENDERSON
J. S. WAGNER PHYSICS DEPT
B. J. WATKINS
T. N. DAVIS
R. PRATHASARATHY
NEAL BROWN

INSTITUTE FOR DEFENSE ANALYSIS
HANS WOLFHARD
ERNEST BAUER

LOWELL, UNIVERSITY OF
G. T. BEST

LOCKHEED MISSILES AND SPACE
COMPANY
JOHN KUMER DEPT 52-54
JOHN B. CLADIS DEPT 52-12
BILLY M. MCCORMAC
DEPT 52-54
TOM JAMES DEPT 52-54
J. B. REAGAN DEPT 52-12
MARTIN WALT DEPT 52-10
RICHARD G. JOHNSON
DEPT 52-12
ROBERT D. SEARS DEPT 52-14

MISSION RESEARCH CORPORATION
D. ARCHER
P. FISCHER
M. SCHEIBE
D. SAPPENFIELD
D. SOWLE

MINNESOTA, UNIVERSITY OF
J. R. WINKLER UNCLAS ONLY

PHOTOMETRIC, INC.
IRVING L. KOFSKY

PHYSICAL DYNAMICS INC.
JOSEPH B. WORKMAN
A. THOMPSON

PHYSICAL SCIENCES, INC.
KURT WRAY
R. L. TAYLOR
G. CALEDONIA

PHYSICS INTERNATIONAL COMPANY
DOC CON FOR TECH LIB

PITTSBURGH, UNIVERSITY OF
WADE L. FITE
MANFRED A. BIONDI
FREDERICK KAUFMAN
EDWARD GERJUOY

PRINCETON UNIV. THE TRUSTEES OF
ARNOLD J. KELLY

R & D ASSOCIATES - CALIFORNIA
RICHARD LATTER
R. G. LINDGREN
BRYAN GABBARD
H. A. DRY
ROBERT E. LELEVIER
R. P. TURCO
ALBERT L. LATTER
FORREST GILMORE
D. DEE

R & D ASSOCIATES - VIRGINIA
HERBERT J. MITCHELL
J.W. ROSENGREN

RAND CORPORATION
CULLEN CRAIN

SCIENCE APPLICATIONS, INC.
DANIEL A. HAMLIN
DAVID SACHS

SPACE DATA CORPORATION
EDWARD ALLEN

STANFORD RESEARCH INSTITUTE
INTERNATIONAL - CALIFORNIA
M. BARON
RAY L. LEADABRAND
WALTER G. CHESTNUT

STANFORD RESEARCH INSTITUTE
INTERNATIONAL - VIRGINIA
WARREN W. BERNING
CHARLES HULBERT

TECHNOLOGY INTERNATIONAL
CORPORATION
W. P. BOQUIST

UNITED TECHNOLOGIES
CORPORATION
H. MICHELS
ROBERT H. BULLIS

UTAH STATE UNIVERSITY
DORAN BAKER
KAY BAKER
C. WYATT
D. BURT

VISIDYNE, INC.
HENRY J. SMITH
J.W. CARPENTER
WILLIAM REIDY
T.C. DEGGES
CHARLES HUMPHREY

WAYNE STATE UNIVERSITY
PIETER K. ROL CHEM
ENGRG & MAT SCI
R.H. KUMMLER

WAYNE STATE UNIVERSITY
DEPT. OF PHYSICS
WALTER KAUPPILA

YALE UNIVERSITY
ENGINEERING DEPARTMENT